UNIVERSITY OF BIRMINGHAM
University of Birmingham Research at Birmingham

# Probing phase evolutions of Au-methyl-propyl-thiolate self-assembled monolayers on Au(111) at molecular level

Gao, Jianzhi; Lin, Haiping; Qin, Xuhui; Zhang, Xin; Ding, Haoxuan; Wang, Yitao; Rokni Fard, Mahroo; Kaya, Dogan; Zhu, Gangqiang; Li, Qing; Pan, Minghu; Guo, Quanmin

*DOI:*
10.1021/acs.jpcb.8b03390

*License:*
Other (please specify with Rights Statement)

*Document Version*
Peer reviewed version

*Citation for published version (Harvard):*
Gao, J, Lin, H, Qin, X, Zhang, X, Ding, H, Wang, Y, Rokni Fard, M, Kaya, D, Zhu, G, Li, Q, Pan, M & Guo, Q 2018, 'Probing phase evolutions of Au-methyl-propyl-thiolate self-assembled monolayers on Au(111) at molecular level', *Journal of Physical Chemistry B*, vol. 122, pp. 6666-6672. https://doi.org/10.1021/acs.jpcb.8b03390

Link to publication on Research at Birmingham portal

**Publisher Rights Statement:**
This document is the unedited Author's version of a Submitted Work that was subsequently accepted for publication in Journal of Physical Chemistry B, copyright © American Chemical Society after peer review. To access the final edited and published work see https://pubs.acs.org/doi/full/10.1021/acs.jpcb.8b03390

**General rights**
Unless a licence is specified above, all rights (including copyright and moral rights) in this document are retained by the authors and/or the copyright holders. The express permission of the copyright holder must be obtained for any use of this material other than for purposes permitted by law.

• Users may freely distribute the URL that is used to identify this publication.
• Users may download and/or print one copy of the publication from the University of Birmingham research portal for the purpose of private study or non-commercial research.
• User may use extracts from the document in line with the concept of 'fair dealing' under the Copyright, Designs and Patents Act 1988 (?)
• Users may not further distribute the material nor use it for the purposes of commercial gain.

Where a licence is displayed above, please note the terms and conditions of the licence govern your use of this document.

When citing, please reference the published version.

**Take down policy**
While the University of Birmingham exercises care and attention in making items available there are rare occasions when an item has been uploaded in error or has been deemed to be commercially or otherwise sensitive.

If you believe that this is the case for this document, please contact UBIRA@lists.bham.ac.uk providing details and we will remove access to the work immediately and investigate.

Download date: 08. Jun. 2020

# Probing Phase Evolutions of Au-Methyl-Propyl-Thiolate Self-Assembled Monolayers on Au(111) at Molecular Level

Jianzhi Gao[†1], Haiping Lin[†2], Xuhui Qin[1], Xin Zhang[3], Haoxuan Ding[4], Yitao Wang[1], Mahroo Rokni Fard[4], Dogan Kaya[4], Gangqiang Zhu*[1], Qing Li[2], Youyong Li[2], Minghu Pan*[3] and Quanmin Guo*[4]

[1] *School of Physics and Information Technology, Shaanxi Normal University, Xi'an 710119, China*

[2]*Institute of Functional Nano & Soft Materials, Jiangsu Key Laboratory for Carbon-Based Functional Materials & Devices, Soochow University, 199 Ren-Ai Road, Suzhou, Jiangsu Province, 215123, China*

[3]*School of Physics, Huazhong University of Science and Technology, Wuhan 430074, China.*

[4]*School of Physics and Astronomy, University of Birmingham, Birmingham B15 2TT, United Kingdom*

[†]These authors contribute equally to this work.

[*] Correspondence and requests for materials should be addressed to Dr G Zhu, email: zgq2006@snnu.edu.cn, Dr. M Pan, email: minghupan@hust.edu.cn and Dr. Q Guo, email: Q.GUO@bham.ac.uk.

## ABSTRACT

A self-assembled monolayer (SAM) consisting of a mixture of $CH_3S$-Au-$SCH_3$, $CH_3S$-Au-$S(CH_2)_2CH_3$ and $CH_3(CH_2)_2S$-Au-$S(CH_2)_2CH_3$ was studied systematically using scanning tunneling microscopy and density functional calculations. We find that the SAM is subject to frequent changes at the molecular level on the time scale of ~minutes. The presence of $CH_3S$ or $CH_3S$-Au as a dissociation product of $CH_3S$-Au-$SCH_3$ plays the key role in the dynamical behavior of the mixed SAM. Slow phase separation takes place at room temperature over hours to days leading to the formation of methyl-thiolate-rich and propyl-thiolate-rich phases. Our results provide new insights into the chemistry of the thiolate-Au interface, especially for ligand exchange reaction in the RS-Au-SR staple motif.

## INTRODUCTION

Alkanethiol passivated gold nanoclusters represent an important class of materials with size-dependent electronic and optical properties.[1-4] Ever since the discovery of thiol-passivated Au nanoclusters,[5] there has been a sustained high level of interest both in producing Au nanoclusters with precise size control and accurate structural determination of such clusters.[6-15] Despite the well-documented stability of thiol-passivated Au nanoclusters, these clusters are found to be able to transform by ligand exchange [16,17] and even intercluster reactions.[15] Many different processes have been proposed to explain ligand exchange and cluster transformation, [18,19] but there is still a lack of consensus over the surface chemistry of the thiolate-Au interface.[20] In particular, when the protecting layer consists of more than one type of thiolates, it is not yet clear how the two different types of thiolates interact with each other and how this interaction affects the stability of the protected Au cluster.

There is a long history of research into self-assembled monolayers (SAM) of alkanethiols on the extended Au(111) surface.[21-58] The fundamental structural motif, the RS-Au-SR staple motif, is found on both Au(111) [23,26] and the surface of Au nanoclusters.[10] Furthermore, the application of scanning tunneling microscopy (STM) to SAMs on Au(111) has a great advantage that it images the surface in real space with atomic scale resolution and is hence able to provide important structural

information of the S-Au interface, which is otherwise difficult to obtain from passivated Au nanoclusters. Here, we present the findings from our recent study of mixed methyl- and propyl-thiolate monolayers on Au(111) using STM. We focus on investigating the mixing and phase-separation of the two alkyl-thiolate species. Our mixed SAM has three different building blocks: $CH_3(CH_2)_2S$-Au-S-$(CH_2)_2CH_3$, $CH_3S$-Au-S-$CH_3$ and $CH_3S$-Au-S-$(CH_2)_2CH_3$. Because of different chain lengths between $CH_3S$ and $CH_3(CH_2)_2S$, ligand exchange reaction can be followed more easily as a result of clear contrast change in STM images. Therefore, *we are able to monitor, on the molecular level, phase evolutions within the* SAM *in real time.*

## EXPERIMENTAL AND COMPUTATIONAL METHODS

The experimental details have been described in an earlier publication.[47] The mixed SAM is prepared by exposing the gold sample to a background of methyl-propyl disulfide (MPDS) vapor at room temperature (RT) at a pressure of $1\times10^{-5}$ mbar. Saturation coverage is reached after ~ 15 minutes' exposure. The exact exposure is subject to uncertainties in the measurement of the MPDS pressure using an ion gauge. The gold sample is a (111)-oriented Au film deposited on a highly-oriented pyrolitic graphite substrate. The Au film is cleaned using cycles of $Ar^+$ ion sputtering and thermal annealing. STM imaging was performed at both RT and 110 K using

electrochemically etched tungsten tips. All STM images reported here, were obtained by using about -0.6 V sample bias and 0.05 nA tunneling current. STM tip is far away from the surface molecules in order to avoid the tip effect. The molecular coverage is obtained by finding the density of the thiolate which is then normalized by the density of surface gold atoms.

The DFT calculations were performed with the Vienna *ab initio* Simulation Package (VASP).[59,60] The electron-ion interactions were described using the projected augmented wave (PAW) method.[61] The exchange-correlation energy was calculated with the general gradient approximation (GGA) functionals of Perdew-Burke-Ernzerhof (PBE).[62] An energy cutoff of 400 eV was selected for the plane-wave expansion. The dispersion corrections of the molecules and Au surface interactions were included by the van der Waals density functional (vdw-DF) proposed by Dion.[63-65] The Au surfaces were modeled with periodic slabs consisting of five atomic layers. A vacuum of 15 Å was adopted to avoid the periodic image interactions normal to the surface. A Monkhorst-Pack grid of 2 × 4 × 1 was employed to sample the surface Brilloun zone. In all cases, the top three layers of atoms were allowed to relax in three dimensions. The first principles STM simulations were conducted with the Tersoff-Hamann method and the bSKAN code. [66, 67]

## RESULTS AND DISCUSSION

### *Full coverage 3 × 4 phase*

We begin by examining the structure of the mixed SAM at the coverage corresponding to 1/3 monolayer (ML) of thiolate (treating both methyl-thiolate and propyl-thiolate equally). Here 1 ML is defined as one thiolate per Au atom. 1/3 ML is thus the maximum coverage that can be achieved on Au(111). Figure 1a and b shows two STM images of the mixed monolayer at RT. It can be seen that complete phase separation into separate methyl-thiolate and propyl-thiolate domains does not happen. The nearly random mixture of methyl-thiolate and propyl-thiolate results in a rather disordered appearance of the STM images. However, as shown previously using Fourier transform of the images,[47] the bright spots in the images have excellent positional correlation and all spots can be matched onto a 3 × 4 lattice which is common for monolayers of methylthiolate,[46,48] ethylthiolate [42,46] and propylthiolate.[55] Previous studies of the 3 × 4 phase of propyl-thiolate SAM [55] and methyl-thiolate SAM,[46] show that the propyl/methyl chains can be divided into two groups as illustrated in the ball model of Fig. 1c. The β chain tilts more towards the surface normal and appears taller than the α chain. Therefore, for the mixed SAM, we expect to see spots in STM images having four different levels of contrast from i) the β

propyl chain; ii) the α propyl chain; iii) the β methyl chain and iv) the α methyl chain. Under our imaging conditions, the "visible" spots in the images from the 3 × 4 phase of the mixed SAM are from either the α or the β propyl chains with the β propyl chain appearing the tallest. The methyl-thiolate species, being significantly shorter than propyl-thiolate, appears dark and "invisible". The 3 × 4 lattice is occupied by a rather random mixture of $CH_3(CH_2)_2S$-Au-S-$(CH_2)_2CH_3$, $CH_3S$-Au-S-$CH_3$ and $CH_3S$-Au-S-$(CH_2)_2CH_3$. This results in the apparent lack of ordering in the two STM images. The images also show the presence of a number of voids within the SAM. These voids are not patches of bare Au(111), otherwise, thiolate from the surrounding area with a high adsorbate density would diffuse into the voids. The lack of ordered structure inside the voids indicates that the voids are filled by $SCH_3$ or Au-$SCH_3$, both are dissociation products of $CH_3S$-Au-S-$CH_3$. $CH_3S$-Au-$SCH_3$ itself is not stable as a complete unit at RT.[68] $SCH_3$ or Au-$SCH_3$ inside the voids are mobile at RT and they provide the required surface pressure to prevent the voids from collapsing.

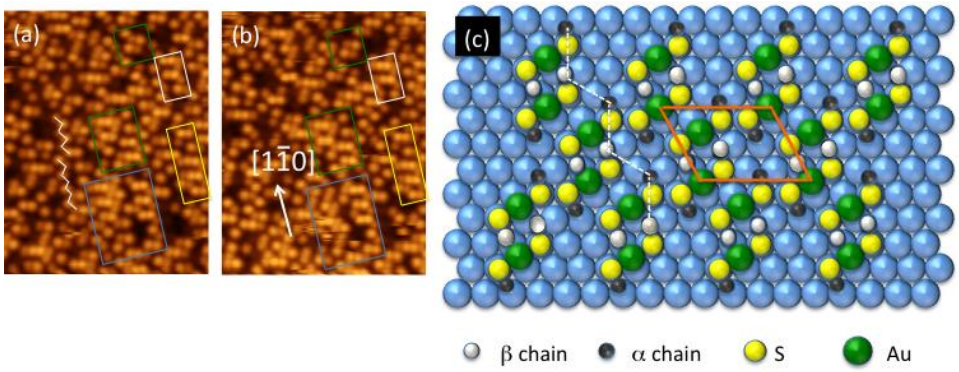



Figure 1. (a) and (b) STM images, 5.5 nm × 7.5 nm, acquired from the same area of the sample at RT. Image in (b) was collected three minutes after the image in (a). Rectangular boxes are drawn onto the images to highlight areas where only minor changes have taken place. Outside the boxes, changes are so extensive that direct comparison between the two images becomes difficult. In both images, the spots are from propyl chains. The brightest spots are the β chains. The methyl chains are in the dark voids and not resolved under the tunnel condition applied. S and Au are not visible in these images. (c) Ball model of the 3 × 4 phase of alkanethiolate monolayers at 1/3 ML coverage. The zigzag line formed by connecting the α and β chains is directly comparable with experimental findings shown in (a).

According to the staple motif, each spot in the STM image comes from one branch of the staple. The $CH_3(CH_2)_2S$-Au-$S(CH_2)_2CH_3$ staple can be identified easily by finding a pair of related spots. For the $CH_3S$-Au-$S(CH_2)_2CH_3$ staple, we can also find the location of the $SCH_3$ branch by knowing where its partner, $S\text{-}(CH_2)_2CH_3$, is located. There are local areas, inside the blue rectangle in Fig. 1a for example, where the composition is significantly rich in propyl-thiolate and the β chains are exclusively propyl chains. Therefore, some minor segregation of propyl-thiolate from the mixed

layer has already taken place.

To summarize the features of the 3 × 4 mixed SAM, most part of the SAM consists of a rather random mixture of $CH_3(CH_2)_2S$-Au-$S(CH_2)_2CH_3$ and $CH_3S$-Au-$S(CH_2)_2CH_3$. Although there are not complete separations of the methyl- and propyl-thiolate, there are local areas enriched either in methyl-thiolate or propyl-thiolate. The areas heavily enriched with methyl-thiolate are covered by a liquid-like $SCH_3$ or $AuSCH_3$ and appear as voids within the 3 × 4 SAM.

When the mixed SAM with the 3 × 4 structure is continuously monitored with the STM, we find that the local areas highly-enriched with propyl-thiolate are more stable and do not change much with time. The two images shown in Fig. 1 are collected from the same area with image in (b) acquired three minutes after that in (a). Significant changes are observed within this three minutes' period. In fact, only a small fraction of the scanned area, mostly regions highly enriched with propyl-thiolate, maintains the original structure. Rectangular boxes are added to the images to assist the eye to identify areas subjected to minor or no changes in between the two scans. The changes can sometimes be captured in real time by the STM as shown in Fig. 2.

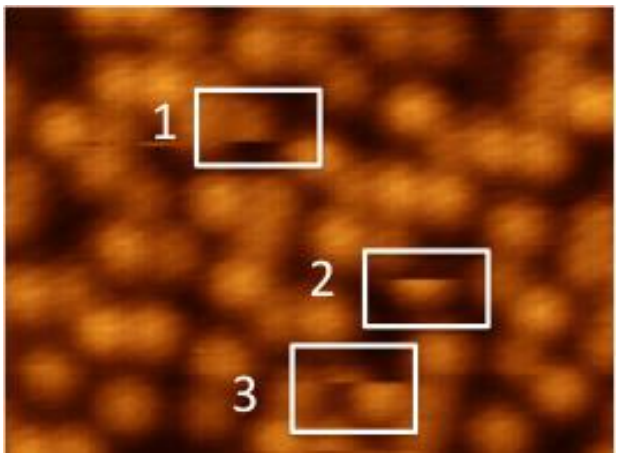



Figure 2. STM image showing real time changes captured by the STM. The fast scan direction is the horizontal direction. After each scan line, the STM tip moves upwards by a small step. Inside the rectangular boxes we highlight instantaneous changes that are recorded by the STM.

Inside rectangular box 1, we see the sudden appearance of a thiolate. We see the top ¾ of the thiolate with the bottom ¼ of it not showing up because the thiolate was not in that location when the tip passed by. This is a typical phenomenon when an atom/molecule moves from somewhere else to a position such that part of the atom/molecule falls in front of the advancing STM tip. Inside box 2, we see a thiolate disappearing after the bottom half of it has been imaged by the STM. In box 3, we can identify a thiolate jumping from its initial location to a new location to the upper left. In this case, the bottom half of the thiolate was seen by the STM in its original location and the top half of the same thiolate seen in the new location.

The events of mobile thiolates shown in Fig. 2 are the ones captured by the STM while in action and are only a small fraction of the total events. When comparing two STM images taken just a few minutes apart, the majority of the thiolates are observed to have changed positions. This high activity of thiolate displacement, however, is not a common feature for the short chain alkanethiol monolayers. When the 3 × 4 phase of a pure propyl-thiolate monolayer [55] or of an ethyl-thiolate monolayer [42,–46] is imaged with the STM at RT, it appears stable with little changes occurring. The facile movement of the propyl and methyl chains inside the mixed SAM is hence a result of the presence of methyl-thiolate. The mobile $AuSCH_3$ and $SCH_3$ are able to interact with $CH_3(CH_2)_2S\text{-}AuS(CH_2)_2CH_3$ and $CH_3(CH_2)_2S\text{-}AuSCH_3$ via ligand exchange reactions. When molecules are observed to change their location or conformation under the STM, there are several potential contributions to these changes. The STM tip, for example, has the capability to initiate changes due to either electronic excitations by the tunneling electrons or the localized electric static force. Under many situations, one can identify which is the dominating contribution to changes by altering the tunneling current of the strength of the electric field beneath the tip. We have not investigated how the observed changes respond to tunnel current or electric field. However, we have clear evidence that the changes are due to the presence of $AuSCH_3$ or $SCH_3$ which are mobile on Au(111) at RT. When the sample temperature

is decreased and the mobility of $AuSCH_3$ or $SCH_3$ is frozen, the molecular layer stops changing.

***Nearly stoichiometric striped phase***

When the mixed layer with the 3 × 4 phase is left at RT in vacuum for two days, there appears to be a gradual decrease in coverage, presumably due to expansion of the monolayer and loss of the thiolate to the surrounding sample holder. There is also a small probability of desorption via the formation of dimethyldisulphide. The 3 × 4 phase eventually becomes disordered before the appearance of a striped phase. Figure 3a shows an STM image acquired at RT showing alternating bright and dim rows of the striped phase. Inset shows the height profile across line A-B. The regular bright-dim row feature can be explained as due to an ordered arrangement of $CH_3S$-Au-$S(CH_2)_2CH_3$. Figure 3c is a structural model derived from DFT calculations and Fig. 3d shows a simulated STM image according to the structural model. The striped phase according to the model consists of 100% $CH_3S$-Au-$S(CH_2)_2CH_3$ staple rows. The staples are organized in such a way that there are alternating $SCH_3$ and $S(CH_2)_2CH_3$ rows, all aligned in the $[11\bar{2}]$ direction. The STM image in Fig. 3a shows that although the overall structure is consistent with the model of Fig. 3c, the real structure at RT is not as rigid. Along the bright $S(CH_2)_2CH_3$ rows, one can see gaps as a result of substitution of $S(CH_2)_2CH_3$ by $SCH_3$. Similarly, along the dim $SCH_3$ rows, we can

find $SCH_3$ being substituted by $S(CH_2)_2CH_3$. Overall, the chemical composition of the striped phase is close to 1:1 for the $SCH_3/S(CH_2)_2CH_3$ ratio. The striped phase shown in Fig. 3 is under dynamical equilibrium at RT. Frequent displacement of thiolate is observed and as a result two subsequent images taken from the same area never look the same. The changes are however limited to the extent that the bright rows remain bright and dim ones remain dim.

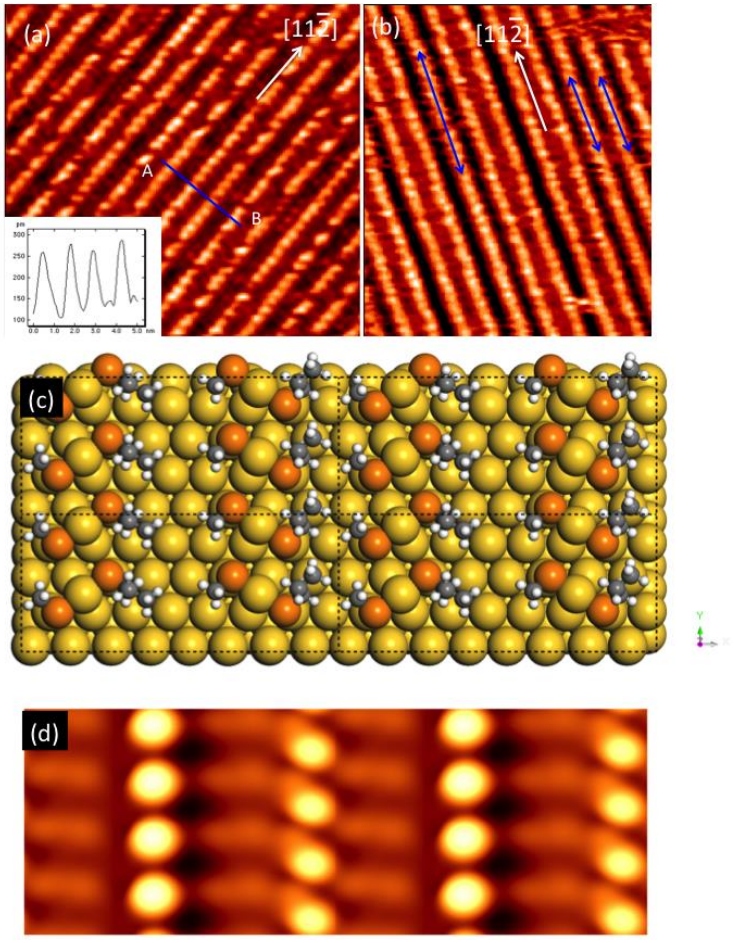



Figure 3. (a) STM image, 10 nm × 10 nm, showing the nearly stoichiometric striped phase with alternating bright and dim rows. There is also evidence of row-pairing. (b) Some rows are not paired

with their neighbors. (c) Structural model derived from DFT. (d) Simulated STM image according to the structural model in (c).

***Striped phases enriched with either $SCH_3$ or $S(CH_2)_2CH_3$***

As described earlier, the nearly stoichiometric striped phase is under dynamic equilibrium. Given enough time, this striped phase changes further leading to clear phase separation. Phase separation gives rise to domains dominated by methyl-thiolate and separate domains dominated by propyl-thiolate. The domains heavily enriched with methyl-thiolate have no ordered structure at RT. However, under repeated scanning by the STM tip, an ordered striped phase can be formed locally as demonstrated in Fig. 4. The formation of the stripes shown in Fig. 4 is tip-induced because once scanning is terminated, the stripes get dissolved quickly into the disordered background. Stripes similar to those shown in Fig. 4 are observed to be stable at lower temperatures. Figure 5a shows an STM image from a striped phase of a methyl-thiolate-rich area at 110 K. Thus, tip-induced striped phase is very similar to the self-formed striped phase under low enough temperature. The reason that the striped phase of methyl-thiolate is not stable at RT is probably due to the entropic effect. When scanning at RT, there is expected to be an attractive tip-molecule interaction. This interaction is electrostatic in nature due to the electric field within the tunnel junction. This attractive interaction tends to pull molecules towards the area below the STM tip. This is equivalent to a compressive pressure acted on the

molecules. This “compressive pressure”, we believe, forces the molecules to assemble into the striped phase.

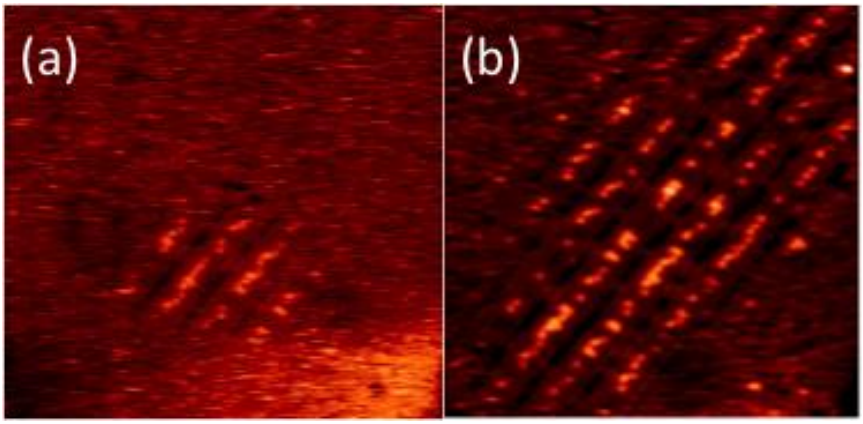



Figure 4. STM-induced formation of a striped phase from a disordered, methyl-thiolate-rich, area at RT. The stripes are parallel to the $[11\bar{2}]$direction. (a) The early stage where four short segments of thiolate rows are formed. (b) Later on, the segments grow longer with new rows also formed. Image size: 20 nm × 20 nm.

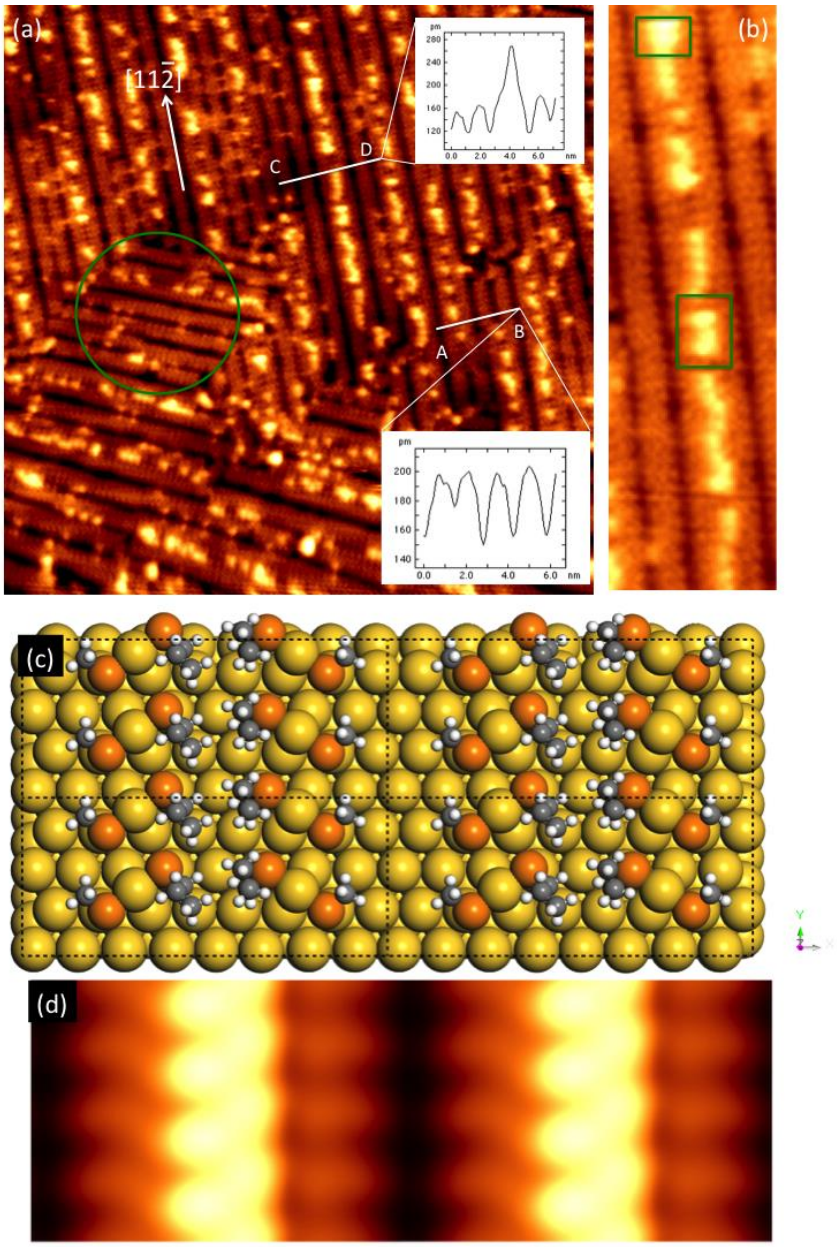



Figure 5. (a) STM image of a striped phase of the mixed SAM. The SAM was prepared at RT and it was cooled down to 110 K. Image was collected at 110 K. The striped phase was formed when temperature is below 190 K. This area is heavily enriched with methyl-thiolate. Insets show height profiles across the staple rows. Area inside the green circle highlights a nearly pure methyl-thiolate phase. (b) β chains of propyl-thiolate appear much taller than the methyl-chains. (c) Structural model derived from DFT calculations. (d) Simulated STM images according to the model in (c).

In Fig. 5a, we first concentrate on a particular area inside the green circle. The height corrugation of the rows, 40 pm, is the same as that found for the $CH_3S$-Au-$SCH_3$ rows. [48] We therefore identify these rows as $CH_3S$-Au-$SCH_3$ rows. The tall features, 120 pm taller than the $CH_3S$-Au-$SCH_3$ rows, are from $S(CH_2)_2CH_3$. The tall features are mostly found in between two rows as shown in Fig. 5b. Figure 5c gives a model based on DFT calculations. According to the model, two adjacent rows are paired with an inter-row distance of 3.5*a*. Each row consists of $CH_3S$-Au-$S(CH_2)_2CH_3$ staples. The $S(CH_2)_2CH_3$ branches from the two rows in the pair have a head-to-head arrangement. Figure 5d shows a simulated STM image according to the model in (c). The simulated image is in good agreement with the experimental findings. For two staple rows in a pair, there are thus two rows of $S(CH_2)_2CH_3$. The experimentally observed images appear more complicated, because the stoichiometry of the staples in each of the paired rows is not necessarily the same. At the top of the image in Fig. 5b, the area inside the green box shows features almost identical to that in Fig. 5c. However, rather than an exact head-to-head $CH_3S$-Au-$S(CH_2)_2CH_3$:$CH_3(CH_2)_2CH_3S$-Au-$SCH_3$ configuration, we find many instances of $CH_3S$-Au-$SCH_3$:$CH_3(CH_2)_2S$-Au-$SCH_3$ and $CH_3S$-Au-$S(CH_2)_2CH_3$:$CH_3S$-Au-$SCH_3$ configurations. Therefore, instead of seeing two regular rows of $S(CH_2)_2CH_3$, we see the frequent interruptions of the $S(CH_2)_2CH_3$ row by $SCH_3$. Figure 6 shows a simulated STM image based on a structural model

allowing the substitution of $S(CH_2)_2CH_3$ by $SCH_3$. The simulated STM image in Fig. 6 is in good agreement with the observed image in Fig. 5a.

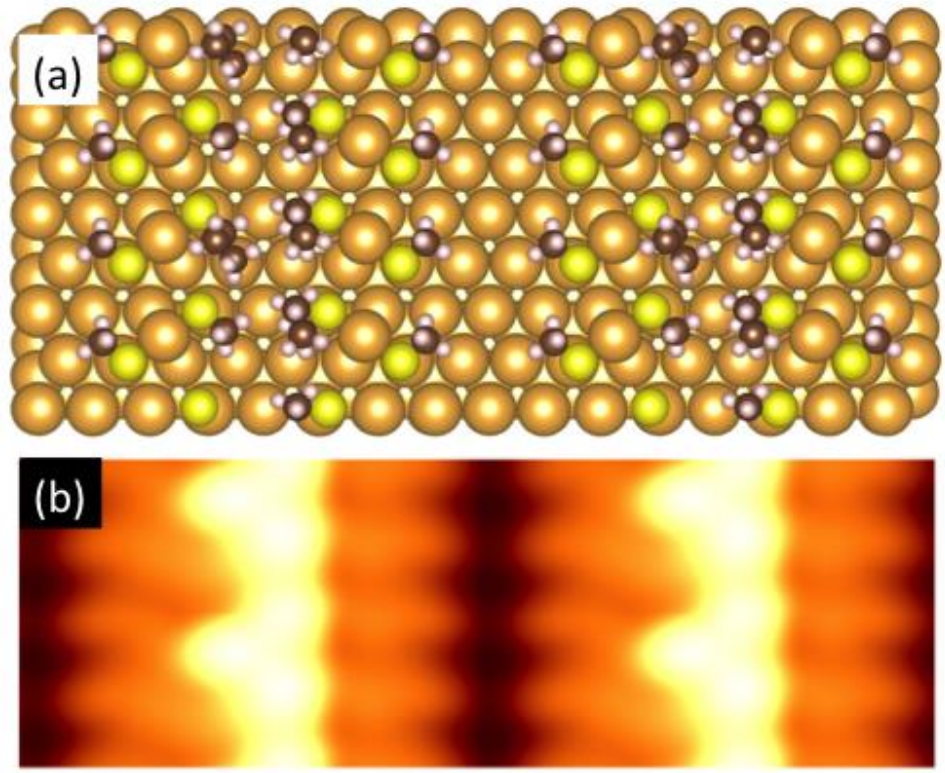



Figure 6. (a) The same structural model as that in Fig. 5c but with the substitution of some $S(CH_2)_2CH_3$ by $SCH_3$. (b) Simulated STM image based on the model in (a).

In areas where propyl-thiolate is the majority of the population, we find striped phases similar to that shown in Fig. 5c even at RT. Figure 7 shows an STM image from an area enriched with propyl-thiolate. The staple rows have similar characteristics as that given by the simulation in Fig. 5c. If we substitute some α $SCH_3$ by $S(CH_2)_2CH_3$ and some β chains by $SCH_3$ in Fig. 5c, the simulated image would be rather similar to that

shown in Fig. 7. It is evident that there is plenty of movement inside the striped SAM of Fig. 7. The $SCH_3/S(CH_2)_2CH_3$ ratio evaluated from Fig. 7 is 4:1. The presence of around 25% of methyl-thiolate is once again responsible for the frequent changes of the propyl-rich SAM observed at RT. We found previously that striped phases of pure propyl-thiolate are stable, not showing displacement of individual thiolate at RT.[47]

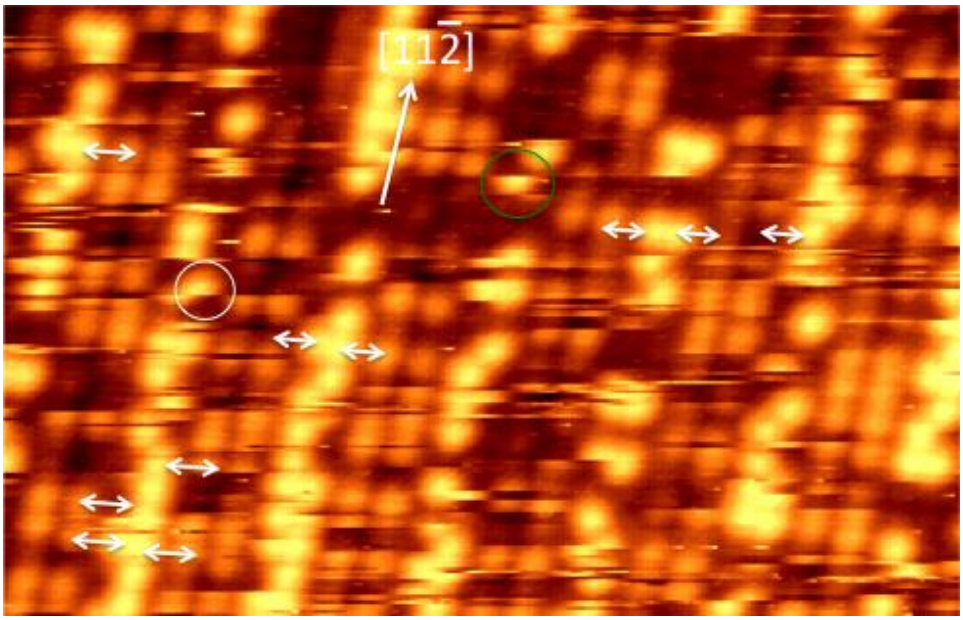



Figure 7. STM image, 12 × 7.5 nm, of a striped phase of staples enriched with propyl-thiolate imaged at RT. The overall striped structure remains more or less unchanged with time, but frequent changes at the individual thiolate level are observed. Arrows indicate two thiolate branches belonging to the same staple. Circles highlight displacement of thiolate as captured by STM in real time.

Our study of the mixed methyl- and propyl-thiolate SAM clearly demonstrates that the SAM is an active layer at room temperature undergoing frequent changes. It has

been known for some time that the gold-thiolate interface is not rigid.[69] When phase separated domains of 1-undecanethiol and 11-mercaptoundecanoic acid are prepared on Au(111), the two thiolate species inter-diffuse and a mixed phase is obtained after several hundred hours at 353 K. [70] Lateral diffusion of thiolates on the surface of gold nano-clusters has also been studied. [71] However, several important questions remain to be answered. What is moving inside a SAM? Does the staple move as a single unit or is the dissociation of the staple a prerequisite for diffusion? If so, is RS-Au or just RS the mobile unit? Our study does not answer all of the above questions. Nevertheless, findings from the present study demonstrate the unequal role of the thiolates. Ligand exchange within the methyl- and propyl-thiolate layer is dominated by the properties of the methyl-thiolate. The methyl-thiolate staple is not stable at RT.[68] The dissociation of the staple should produce RS-Au, RS and even free Au adatoms. These dissociation products can then attack the $CH_3(CH_2)_2S$-Au-$S(CH_2)_2CH_3$ staple leading to ligand exchange. Of course, at high enough temperatures, the $CH_3(CH_2)_2S$-Au-$S(CH_2)_2CH_3$ staple is expected to break as well. Loss of methyl-thiolate from the surface through thermal desorption also takes place at high enough temperatures leading to the formation a pure propyl-thiolate SAM.[55] Although the S-Au bond within the staple can be broken via thermal activation, the energy required to break this bond increases with the chain length of the alkanthiol.

For longer chain lengths, the van der Waals interaction provides a restoring force to repair the broken S-Au bond before the complete separation of RS chain from the staple. This restoring force is most effective for SAMs on the flat Au(111) surface, but less effective on the surface of nanoclusters. This is because on the surface of nanoclusters, the curved surface of the cluster is unable to keep a uniform distance between adjacent alkyl-thiolate chains, hence a weakened Van der Waals force.

The STM as an imaging technique has its drawbacks that each image requires a rather lengthy time to collect. This makes the STM unsuitable to follow changes that occur too rapidly. There are, however, ways to overcome this shortcoming. For example, by recording tunnel current as a function of time with the feedback loop disabled, temporal resolution of the order of 20 $\mu s$ has been achieved [72] when studying the system of decanethiol monolayers on Au(111).[73]

## CONCLUSIONS

The interaction of short chain alkanethiols including $CH_3SH$, $CH_3CH_2SH$ and $CH_3(CH_2)_2SH$ with the Au(111) surface produces similar structures based on the RS-Au-SR staple motif. They all have an ultimate 3 × 4 phase at 1/3 ML of coverage. At coverage below 1/3 ML, the SAMs organize into similar striped phases. Among the three Au-thiolate staples we have investigated so far, $CH_3(CH_2)_2S$-Au-$S(CH_2)_2CH_3$ is the most stable. The methyl-thiolate SAM has the lowest stability. By adding methyl-

thiolate into propyl-thiolate, a mixed 3 × 4 phase containing nearly equal amount of $SCH_3$ and $SCH_3(CH_2)_2$ is formed at 1/3 ML at RT. $CH_3S$-Au-$SCH_3$ readily breaks apart at RT giving rise to $SCH_3$ and $AuSCH_3$. It is not clear if we have both $SCH_3$ and $AuSCH_3$ on the surface or just $SCH_3$. What is clear is that $SCH_3$ or $AuSCH_3$ is mobile on the surface and can react with $CH_3(CH_2)_2S$-Au-$S(CH_2)_2CH_3$ by the ligand exchange process. This ligand exchange makes the SAM in dynamical equilibrium at RT. The mixed SAM when left at RT in vacuum slowly phase separates into methyl-thiolate-rich and propyl-thiolate-rich domains. The phase separation however, does not produce either a pure methyl-thiolate phase or a pure propyl-thiolate phase.

**Acknowledgements**

This work was financially supported by the National Science Foundation of China (Grant no. 11604196) and Fundamental Research Funds for the Central Universities (Grant no. GK201801005). J. Gao thanks for the support of National Demonstration Center for Experimental X-physics Education (Shaanxi Normal University).

## REFERENCES


[1] Zhu, M.; Aikens, C. M.; Hollander, F. J.; Schatz, G. C.; Jin, R. Correlating the crystal structure of a thiol-protected $Au_{25}$ cluster and optical properties. *J. Am. Chem. Soc*. **2008**, *130*, 5883-5885.

[2] Weissker, H. C. *et al*. Information on quantum states pervades the visible spectrum of the ubiquitous $Au_{144}(SR)_{60}$ gold nanocluster. *Nat. Commun*. **2014**, *5*, 3785.

[3] Philip, R.; Chantharasupawong, P.; Qian, H. F.; Jin, R. C.; Thomas, J. Evolution of nonlinear optical properties: From gold atomic clusters to plasmonic nanocrystals. *Nano Lett*. **2012**, *12*, 4661-4667.

[4] Negishi, Y *et al*. A Critical size for emergence of nonbulk electronic and geometric structures in dodecanethiolate-protected Au clusters. *J. Am. Chem. Soc*. **2015**, *137*, 1206-1212.

[5] Brust, M.; Fink, J.; Bethell, D.; Schiffrin, D. J. Synthesis and reactions of functionalised gold nanoparticles, *J. Chem. Soc. Commun*. **1995**, *16*, 1655-1156.

[6] Hasan, M.; Bethall, D.; Brust, M. The fate of sulfur-bound hydrogen on formation of self-assembled thiol monolayers on gold: $^{1}H$ NMR spectroscopic evidence from solutions of gold clusters. *J. Am. Chem. Soc*. **2002**, *124*, 1132-1133.

[7] Badia, A.; Cuccia, L.; Demers, L.; Morin, F.; Lennox, R. B. Structure and dynamics in alkanethiolate monolayers self-assembled on gold nanoparticles: a DSC, FT-IR and deuterium NMR study. *J. Am. Chem. Soc*. **1997**, *119*, 2682-2692.

[8] Sardar, R.; Shumaker-Parry, J. S. Spectroscopic and microscopic investigation of gold nanoparticle formation: Ligand and temperature effects on rate and particle size. *J. Am. Chem. Soc*. **2011**, *133*, 8179-8190.

[9] Dass, A.; Theivendran, S.; Nimmala, P. R.; Kumara, C.; Jupally, V. R.; Fortunelli, A.; Barcaro, G.; Zuo, X.; Noll, B. C. $Au_{133}(SPh\text{-}tBu)_{52}$ nanomolecules:X-ray crystallography, optical, electrochemical, and theoretical analysis. *J. Am. Chem. Soc.* **2015**, *137*, 4610-4163.

[10] Jadzinsky, P. D.; Careo, G.; Ackerson, C.J.; Bushnell, D. A.; Kornberg, R. D. Structure of a thiol monolayer-protected gold nanoparticle at 1.1 angstrom resolution. *Science* **2007**, *318*, 430-433.

[11] Jensen, K. M. O.; Juhas, P.; Tofanelli, M. A.; Heinecke, C. L.; Vauhgan, G.; Ackerson, C. J.; Billinge, S. J. L. Polymorphism in magic-sized $Au_{144}(SR)_{60}$ clusters.

*Nat. Comm*. **2016**, 7, 11859.
[12] Zeng, C.; Chen, Y.; Iida, K.; Nobusada, K.; Kirschbaum, K.; Lambright, K. J.; Jin, R. Gold quantum boxes: On the periodicities and the quantum confinement in the $Au_{28}$, $Au_{36}$, $Au_{44}$, and $Au_{52}$ magic series. *J. Am. Chem. Soc*. **2016**, *138*, 3950-3953.
[13] Fernando, A.; Aikens, C. M. Deciphering the ligand exchange process on thiolate monolayer protected $Au_{38}(SR)_{24}$ nanoclusters. *J. Phys. Chem. C*. **2016**, *120*, 14948-14961.
[14] Zeng, C.; Liu, C.; Chen, Y.; Rosi, N.; Jin, R. Atomic structure of self-assembled monolayer of thiolates on a tetragonal $Au_{92}$ nanocrystal, *J. Am. Chem. Soc*. **2016**, *138*, 8710-8713.
[15] Krishnadas, K. R.; Ghosh, A.; Baksi, A.; Chakraborty, I.; Natarajan, G.; Pradeep, T. Intercluster reactions between $Au_{25}(SR)_{18}$ and $Ag_{44}(SR)_{30}$. *J. Am. Chem. Soc*. **2016**, *138*, 140-148.
[16] Ingram, R. S.; Hostetler, M. J.; Murray, R. W. Poly-hetero-ω-functionalized alkanethiolate-stabilized gold cluster compounds. *J. Am. Chem. Soc*. **1997**, *119*, 9175-9178.
[17] Imabayashi, S.; Hobara, D.; Kakiuchi, T. Voltammetric detection of the surface diffusion of adsorbed thiolate molecules in artificially phase-separated binary self-assembled monolayers on a Au (111) surface. *Langmuir* **2001**, *17*, 2560-2563.
[18] Heinecke, C. L.; Ni, T. W.; Malola, S.; Makinen, V.; Wong, O. A.; Kakkinen, H.; Ackerson, C. J. Structural and theoretical basis for ligand exchange on thiolate monolayer protected gold nanoclusters. *J. Am. Chem. Soc*. **2012**, *134*, 13316-13322.
[19] Niihori, Y.; Kurashige, W.; Matsuzaki, M.; Negishi, Y. Remarkable enhancement in ligand-exchange reactivity of thiolate-protected Au 25 nanoclusters by single Pd atom doping. *Nanoscale* **2013**, *5*, 508-512.
[20] Burgi, T. Properties of the gold–sulphur interface: from self-assembled monolayers to clusters. *Nanoscale* **2015**, *7*, 15553-15567.
[21] Love, J. C.; Estroff, L. A.; Kriebel, J. K.; Nuzzo, R. G.; Whitesides, G. M. Self-assembled monolayers of thiolates on metals as a form of nanotechnology. *Chem. Rev*. **2005**, *105*, 1103-1170.
[22] Kind, M.; Wöll, Ch. Organic surfaces exposed by self-assembled organothiol monolayers: Preparation, characterization, and application. *Prog. Surf. Sci*. **2009**, *84*, 230-278.

[23] Maksymovych, P.; Voznyy, O.; Dougherty, D. B.; Sorescu, D. V.; Yates, J. T. Jr. Gold adatom as a key structural component in self-assembled monolayers of organosulfur molecules on Au (111). *Prog. Surf. Sci*. **2010**, *85*, 206-240.
[24] Schreiber, F. Structure and growth of self-assembling monolayers. *Prog. Surf. Sc*i. **2000**, *65*, 151-257.
[25] Vericat, C.; Vela, M. E.; Benitez, G.; Carro, P.; Salvarezza, R. C. Self-assembled monolayers of thiols and dithiols on gold: new challenges for a well-known system. *Chem. Soc. Rev*. **2010**, *39*, 1805-1834.
[26] Guo, Q.; Li, F-S. Self-assembled alkanethiol monolayers on gold surfaces: resolving the complex structure at the interface by STM. *Phys. Chem. Chem. Phys*. **2014**, *16*, 19074-19090.
[27] Poirier, G. E. Coverage-dependent phases and phase stability of decanethiol on Au (111). *Langmuir* **1999**, *15*, 1167-1175.
[28] Vargas, M. C.; Giannozzi, P.; Selloni, A.; Scoles, G. Coverage-dependent adsorption of $CH_3S$ and $(CH_3S)_2$ on Au(111): a density functional theory study. *J. Phys. Chem. B.* **2001**, *105*, 9509-9513.
[29] Ulman, A. Formation and structure of self-assembled monolayers. *Chem. Rev.* **1996**, *96*, 1533-1554.
[30] Poirier, G. E. Characterization of organosulfur molecular monolayers on Au (111) using scanning tunneling microscopy. *Chem. Rev*. **1997**, *97*, 1117-1128.
[31] Kondoh, H.; Iwasaki, M.; Shimada, T.; Amemiya, K.; Yokoyama, T.; Ohta, T.; Shimomura, M.; Kono, S. Adsorption of thiolates to singly coordinated sites on Au (111) evidenced by photoelectron diffraction. *Phys. Rev. Lett*. **2003**, *90*, 066102.
[32] Toerker, M.; Staub, R.; Fritz, T.; Schmitz-Hubsch, T.; Sellam, F.; Leo, K. Annealed decanethiol monolayers on Au (111)–intermediate phases between structures with high and low molecular surface density. *Surf. Sci*. **2000**, *445*, 100-108.
[33] Nuzzo, R. G.; Dubois, L.H.; Allara, D. L. Fundamental studies of microscopic wetting on organic surfaces. 1. Formation and structural characterization of a self-consistent series of polyfunctional organic monolayers. *J. Am. Chem. Soc.* **1990**, *112*, 558-569.
[34] Chidsey, C. E. D.; Liu, G.-Y.; Rowntree, P.; Scoles, G. Molecular order at the surface of an organic monolayer studied by low energy helium diffraction. *J. Chem. Phys.* **1989**, *91*, 4421-4423.

[35] Dishner, M. H.; Hemminger, J. C.; Feher, F. J. Direct observation of substrate influence on chemisorption of methanethiol adsorbed from the gas phase onto the reconstructed Au (111) surface. *Langmuir* **1997**, *13*, 2318-2322.
[36] Dubois, L. H.; Zegarski, B. R.; Nuzzo, R. J. Molecular ordering of organosulfur compounds on Au (111) and Au (100): Adsorption from solution and in ultrahigh vacuum. *J. Chem. Phys.* **1993**, *98*, 678-688.
[37] Camillone, N.; Leung, T. Y. B.; Schwartz, P.; Eisenberger, P.; Scoles, G. Chain length dependence of the striped phases of alkanethiol monolayers self-assembled on Au (111): An atomic beam diffraction study. *Langmuir* **1996**, *12*, 2737-2746.
[38] Fenter, P.; Eberhardt, A.; Eisenberger, P. Self-assembly of n-alkyl thiols as disulfides on Au (111), *Science* **1994**, *266*, 1216-1218.
[39] Maksymovych, P.; Sorescu, D. C.; Yates, Jr. J. T. Gold-adatom-mediated bonding in self-assembled short-chain alkanethiolate species on the Au (111) surface. *Phys. Rev. Lett.* **2006**, *97*, 146103.
[40] Maksymovych, P.; Yates, Jr. J. T. Au adatoms in self-assembly of benzenethiol on the Au (111) surface. *J. Am. Chem. Soc.* **2008**, *130*, 7518-7519.
[41] Li, F.; Zhou, W-C.; Guo, Q. Uncovering the hidden gold atoms in a self-assembled monolayer of alkanethiol molecules on Au (111). *Phys. Rev. B.* **2009**, *79*, 113412.
[42] Li, F.; Tang, L.; Voznyy, O.; Gao, J.; Guo, Q. The striped phases of ethylthiolate monolayers on the Au (111) surface: a scanning tunneling microscopy study. *J. Chem. Phys.* **2013**, *138*, 194707.
[43] Li, F.; Tang, L.; Zhou, W-C.; Guo, Q. Adsorption and electron-induced dissociation of ethanethiol on Au (111). *Langmuir* **2012**, *28* (30), 11115-11120.
[44] Li, F.; Tang, L.; Zhou, W-C.; Guo, Q. Relationship between the c (4× 2) and the ($\sqrt{3}\times\sqrt{3}$) R30° phases in alkanethiol self-assembled monolayers on Au (111). *Phys. Chem. Chem. Phys.* **2011**, *13* (25), 11958-11964.
[45] Li, F.; Tang, L.; Zhou, W-C.; Guo, Q. Adsorption site determination for Au-octanethiolate on Au (111). *Langmuir* **2010**, *26*, 9484-9490.
[46] Tang, L.; Li, F.; Zhou, W-C.; Guo, Q. The structure of methylthiolate and ethylthiolate monolayers on Au (111): Absence of the ($\sqrt{3}\times\sqrt{3}$) R30 phase. *Surf. Sci.* **2012**, *606*, L31-L35.
[47] Gao, J.; Li, F.; Guo, Q. Mixed methyl-and propyl-thiolate monolayers on a Au (111) Surface. *Langmuir* **2013**, *29*, 11082-11086.

[48] Tang, L.; Li, F.; Guo, Q. Complete structural phases for self-assembled methylthiolate monolayers on Au (111). *J. Phys. Chem. C*. **2013**, *117*, 21234-21244.
[49] Mazzarello, R.; Cossaro, A.; Verdini, A.; Rousseau, R.; Casalis, L.; Danisman, M. F.; Floreano, L.; Scandolo, S.; Morgante, A.; Scoles, G. Structure of a $CH_3S$ monolayer on Au(111) solved by the interplay between molecular dynamics calculations and diffraction measurements. *Phys. Rev. Lett*. **2007**, *98*, 016102.
[50] Wang, Y.; Chi, Q.; Hush, N. S.; Reimers, J. R.; Zhang, J.; Ulstrup. J. Scanning tunneling microscopic observation of adatom-mediated motifs on gold− thiol self-assembled monolayers at high coverage. *J. Phys. Chem. C.* **2009**, *113*, 19601-19608.
[51] Yu, M.; Bovet, N.; Satterley, C. J. *et al*. True nature of an archetypal self-assembly system: Mobile Au-thiolate species on Au (111). *Phys. Rev. Lett*. **2006**, *97*, 166102.
[52] Jiang, D. E.; Dai, S. Cis-trans conversion of the $CH_3S$-Au-$SCH_3$ complex on Au(111). *Phys. Chem. Chem. Phys*. **2009**, *11*, 8601-8605.
[53] Hauptmann, N.; Robles, R.; Abufager, P.; Lorente, N.; Berndt, R. AFM imaging of mercaptobenzoic acid on Au(110): Submolecular contrast with metal tips. *J. Phys. Chem. Lett*. **2016**, *7*, 1984-1997.
[54] Hakkinen, H. The gold-sulfur interface at the nanoscale, *Nat. Chem*. **2012**, *4*, 443.
[55] Gao, J., Li, F. S., Guo, Q. Balance of forces in self-assembled monolayers. *J. Phys. Chem. C.* **2013**, *117*, 24985-24990.
[56] Maksymovych, P.; Yates, J. T. Jr. Au adatoms in self-assembly of benzenethiol on the Au(111) surface. *J. Am. Chem. Soc*. **2008**, *130*, 7518-7519.
[57] Heister, K.; Allara, D.; Bahnck, K.; Frey, S.; Zharnikov, M.; Gruze, M. Deviations from 1:1 compositions in self-assembled monolayers formed from adsorption of asymmetric dialkyl disulfides on gold. *Langmuir* **1999**, *15*, 5440-5443.
[58] Maksymovych, P.; Sorescu, D. C.; Voznyy, O.; Yates, J. T. Jr. Hybridization of phenylthiolate- and methylthiolate-adatom species at low coverage on the Au(111) surface. *J. Am. Chem. So*c. **2013**, *135*, 4922-4925.
[59] Kresse, G.; Hafner, J. *Ab initio* molecular dynamics for open-shell transition metals. *Phys. Rev. B* **1993**, 48, 13115.
[60] Kresse, G.; Hafner, J., *Ab initio* molecular-dynamics simulation of the liquid-metal-amorphous-semiconductor transition in germanium. *Phys. Rev. B* **1994**, 49, 14251.

[61] Kresse, G.; Joubert, D., From ultrasoft pseudopotentials to the projector augmented-wave method. *Phys. Rev. B* **1999**, 59, 1758.
[62] Elmér, R.; Berg, M.; Carlén, L.; Jakobsson, B.; Norén, B.; Oskarsson, A.; Ericsson, G.; Julien, J.; Thorsteinsen, T. F.; Guttormsen, M. *et al.* $K^+$ Emission in symmetric heavy ion reactions at subthreshold energies. *Phys. Rev. Lett.* **1996**, 77, 4884.
[63] Dion, M.; Rydberg, H.; Schröder, E.; Langreth, D. C.; Lundqvist, B. I. Van der Waals density functional for general geometries, *Phys. Rev. Lett.* **2004**, 92, 246401.
[64] Kong, L.; Román-Pérez, G.; Soler, J. M. Energetics and dynamics of $H_2$ adsorbed in a nanoporous material at low temperature. *Phys. Rev. Lett.* **2009**, 103, 096102.
[65] Klimeš, J.; Bowler, D. R. Van der Waals density functionals applied to solids. *Phys. Rev. B* **2011**, 83, 195131.
[66] Tersoff, J. Role of tip electronic structure in scanning tunneling microscope images, *Phys. Rev. B* **1990,** 41, 1235.
[67] Hofer, W. A.; Foster, A. S.; Shluger, A. L. Theories of scanning probe microscopes at the atomic scale. *Reviews of Modern Physics* **2003**, *75*, 1287.
[68] Hu, G.X.; Jin, R.C.; Jiang, De-en. Beyond the staple motif: a new order at the thiolate–gold interface**.** *Nanoscale*, **2016**, 8, 20103-20110.
[69] Smith, R. K.; Reed, S. M.; Lewis, P. A.; Monnell, J. D.; Weiss, P. S. Phase separation within a binary self-assembled monolayer on Au {111} driven by an amide-containing alkanethiol. *J. Phys. Chem. B*, **2001**, *105*, 1119-1122.
[70] Imabayashi, S.; Hobara, D.; Kakiuchi, T. Voltammetric detection of the surface diffusion of adsorbed thiolate molecules in artificially phase-separated binary self-assembled monolayers on a Au(111) surface. *Langmuir*, **2001**, *17*, 2560-2563.
[71] Yulikov, M.; Lueders, P.; Warsi, M. F.; Chchik, V.; Jeschke, G. Distance measurements in Au nanoparticles functionalized with nitroxide radicals and Gd(3+)-DTPA chelate complexes. *Phys. Chem. Chem. Phys.* **2012**, *14*, 10732-10746.
[72] Wu, H.; Sotthewes, K.; Kumar, A.; Vancso, J. G.; Schon, P. M.; Zandvliet, H. J. W. Dynamics of decanethiol self-assembled monolayers on Au(111) studied by time-resolved scanning tunneling microscope. *Langmuir*, **2013**, *29*, 2250-2257.
[73] Sotthewes, K.; Wu, H.; Kumar, A.; Vancso, J. G.; Schon, P. M.; Zandvliet, H. J. W. Molecular dynamics and energy landscape of decanethiolates in self-assembled monolayers on Au(111) studied by scanning tunneling microscopy. *Langmuir*, **2013**,

Formatted: Font: Italic
Formatted: Font: Bold
Formatted: Font: Italic
Formatted: Font: Bold

*29*, 3662-3667.

Formatted: Font: Italic

TOC Graphic

